Biomimetic Doxorubicin Loaded Polymersomes from Hyaluronan-*block*-Poly(γ-benzyl glutamate) Copolymers

K. Kumar Upadhyay,[†,‡,§] J.-F. Le Meins,[†,‡] A. Misra,[§] P. Voisin,[||] V. Bouchaud,[||] E. Ibarboure,[†,‡] C. Schatz,[†,‡] and S. Lecommandoux*[,†,‡]

Université de Bordeaux, UMR5629, ENSCPB, 16, Avenue Pey Berland, 33607 Pessac-Cedex, France, CNRS, Laboratoire de Chimie des Polymères Organiques, UMR5629, Pessac, France, Pharmacy Department, Faculty of Technology and Engineering, Kalabhavan, Maharaja Sayajirao University of Baroda, Vadodara-390001, Gujarat state, India, and Université de Bordeaux, Laboratoire de Résonance Magnétique des Systèmes Biologiques UMR 5536 CNRS, 146, rue Léo Saignat - Case 93 33076 Bordeaux, France

Received June 8, 2009; Revised Manuscript Received July 15, 2009

Using "click chemistry" as an easy and versatile synthetic strategy to combine hyaluronan and polyglutamate blocks, we have prepared nanovesicles (polymersomes) that present a controlled size, excellent colloidal stability, and a high loading capacity for hydrophilic and hydrophobic drugs. The unique feature of our concept is the use of hyaluronan, a polysaccharide with known capacity for targeting cancer-related protein receptors, as the hydrophilic portion of a block copolymer system. The cytotoxicity and internalization mechanism of doxorubicin-loaded polymersomes have been evaluated in C6 glioma tumor cell lines. The dual purpose served by hyaluronan, as both a hydrophilic block critical to vesicle formation and a binding agent for biological targets, breaks new ground in terms of multifunctional nanomaterial design for drug delivery.

Introduction

Nanotechnology is an exciting approach to the development of new therapeutics, expected to change the landscape for pharmaceutical companies.[1,2] In this context, block copolymer vesicles are considered as promising drug delivery systems, mainly due to high membrane stability that overcomes most of the challenges encountered with similarly structured liposomes.[3−7] The chemical versatility of block copolymers offers the additional advantage of almost infinite possibilities for the introduction of a specific biofunctionality with properties targeting a defined disease.[8−13] In addition to a high drug loading capacity and an adequate stability in bloodstream circulation, the capacity of a colloidal drug delivery system to selectively accumulate the drug at the site of action is of major importance to improve therapeutic efficiency and reduce side effects.[14,15] A large range of targeting ligands such as antibodies, peptides, nucleic acids, and carbohydrates have now been identified to selectively bind biological targets. However, integration of these binding agents onto nanocarriers often requires tedious chemical reactions and decreases the nanoparticle stability and, as a consequence, blood half-life. The originality of our strategy consists of using a polymer moiety that acts as a bioreceptor and a stabilizing agent in the nanoparticle construction. Hyaluronan, a linear glycosaminoglycan consisting of alternating D-glucuronic acid and *N*-acetyl D-glucosamine units has been selected for both its physicochemical and biological properties. Hyaluronan is a highly water-soluble polymer due to its polyelectrolyte behavior and acts thus as an efficient electrosteric stabilizer when grafted at the surface of nanoparticles. More importantly, hyaluronan is known as a major ligand for CD44, a type 1 transmembrane glycoprotein upregulated in certain cancers.[16] Targeting to CD44 with hyaluronan or anti-CD44 antibodies grafted onto nanocarrier systems such as liposomes has been performed by several authors for cancer therapies.[17−19] However, drawbacks related to liposome surface chemistry include a restricted chemical accessibility and a multipoint attachment of the HYA to the surface when coupling was performed covalently via glucuronic carboxylates.

Additionally, lipid-based vesicles generally present the major disadvantage of poor stability in physiological conditions, even if recent examples of vesicles based on pegylated lipids show improved properties.[20,21] However, surface functionalization with targeting moieties such as hyaluronan even further compromises their colloidal stability and their use in vivo. Polymer vesicles can overcome this main challenge and have been demonstrated to act as robust containers[22,23] able to encapsulate both hydrophilic and hydrophobic molecules.[24] Indeed, their membrane physical properties are directly correlated to their thickness, which can be controlled by the block copolymer molecular weight. Among the different block copolymer vesicles studied so far, polypeptide-based vesicles present several advantages. Their building blocks, which are biocompatible by nature, mimic the behavior of proteins and drive the self-assembly process with accurate control of their secondary structure. For example, it has been shown that vesicles can be highly stabilized due to the rod-like conformation of polypeptide chains forming the hydrophobic part of the membrane.[25,26] In recent and relevant work, Deming and coworkers reported the formation of poly(L-lysine)-*block*-poly(arginine) block copolymers.[27] Interestingly, the poly(arginine) segment was used both to direct structure for vesicle formation and to provide biofunctionality for efficient intracellular delivery

* To whom correspondence should be addressed. E-mail: lecommandoux@enscpb.fr.
† Université de Bordeaux, UMR5629.
‡ CNRS, Laboratoire de Chimie des Polymères Organiques.
§ Maharaja Sayajirao University of Baroda.
|| Université de Bordeaux, Laboratoire de Résonance Magnétique des Systèmes Biologiques UMR 5536 CNRS.

10.1021/bm9006419 CCC: $40.75
Published on Web 08/05/2009

of the vesicles, mimicking the arginine-rich sequence identified as relevant in protein-transduction domains.[28]

Experimental Section

Materials. Hyaluronan was purchased from Life core company ($\bar{M}_w$ = 5140 g/mol, Ip = 1.41) and was characterized by ^{1}H NMR in D_20, static light scattering measurements, and gel permeation chromatography (GPC) in aqueous acetic acid buffer (pH 5.6). γ-Benzyl-L-glutamate *N*-carboxyanhydride (NCA-BLG) was purchased from Isochem (France) and used as received. Dimethylsulfoxide (DMSO) was purchased from Baker and was stirred overnight over CaH_2 and distilled prior to use. All other reagents were purchased from Sigma Aldrich. Sodium cyanoborohydride ($NaCNBH_3$, 98%), copper (I) bromide (CuBr, 98%), *N*,*N*,*N*′,*N*′,*N*″-pentamethyldiethylenetriamine (PMDETA, 99%), and propargylamine (+98%) were used as received. Doxorubicin hydrochloride was purchased from RPG Life Sciences Limited, Mumbai (India).

Synthetic Procedures. *Preparation of* α*-Azido Poly(*γ*-benzyl* L*-glutamate) (N_3-PBLG).* Detailed information about the synthetic and characterization procedures can be found in refs 30−32. We obtained a PBLG of $\bar{M}_n$ = 5000 g/mol with a polydispersity index of 1.1.

Preparation of α*-Alkyne-HYA by Reductive Amination.* The synthetic strategy was based on a coupling reaction between poly(γ-benzyl L-glutamate) (PBLG) and hyaluronan (HYA) using a click chemistry process. For that purpose, PBLG was end-functionalized by an azide group according to a procedure previously described by our group,[32] and hyaluronan by an alkyne function. Conventional reductive amination was chosen to couple reducing end of hyaluronan with propargylamine, using sodium cyanoborohydride ($NaCNBH_3$) as a reducing agent. The reaction was carried out in acetate buffer at room temperature. In detail, sodium hyaluronan (2.2 g, 0.60 mmol) was solubilized in acetate buffer pH = 5.6, at 2% w/w. 2.82 mL of propargylamine (∼75 equiv) was added under magnetic stirring. Then, 2.77 g of $NaCNBH_3$ (44 mmol, ∼75 equiv) was added and the mixture was stirred for 5 days at 50 °C. Subsequently, the mixture was concentrated under vacuum, precipitated in cold methanol (400 mL), collected by centrifugation, and washed with cold methanol (100 mL) to remove excess of propargylamine and sodium cyanoborohydride. Then, the product was dried under vacuum. The reaction is quantitative (∼100% yield). For the click reaction with PBLG, sodium hyaluronan was first acidified by adding HCl, so as to be fully soluble in DMSO, the solvent used for the reaction.

Synthesis of Hyaluronan-b-poly(γ*-benzyl-*L*-glutamate) by Huisgen's 1,3-Dipolar Cycloaddition ("click" chemistry).* Huisgen's 1,3-dipolar cycloaddition (click reaction) was performed in DMSO at 60 °C using CuBr as the catalyst and pentamethyldiethylenetriamine (PMDETA) as a ligand. After 48 h of reaction, click chemistry afforded the targeted PBLG-*b*-HYA block copolymers as illustrated in Scheme 1. Experimentally, N_3-PBLG (1.05 g, 210 μmol, 1 equiv) and α-alkyne-HYA (2.1 g, 410 μmol, 2 equiv) were solubilized in a flask containing 70 mL of anhydrous DMSO. The mixture was stirred for 20 min and PMDETA (87.04 μL, 420 μmol, 2 equiv) was added through sterile syringe under nitrogen environment. The mixture was degassed by three freeze−thaw cycles and added in another Schlenk containing CuBr (60 mg, 420 μmol, 2 equiv) via nitrogen-purged syringe. The Schlenk flask was placed in an oil bath regulated at 60 °C for 2 days under static nitrogen pressure. The excess of HYA was removed from the block copolymers by extensive dialysis (MWCO 50 000 g/mol) against water at pH = 3.5 to keep the polysaccharide in its acidic form. The block copolymer which progressively precipitates during dialysis was collected through centrifugation and dried under vacuum. After weighing the obtained powder, the final yield was 65%. The copolymer was analyzed by ^{1}H NMR, IR spectroscopy, and GPC. The triazole proton peak was found at 7.6 ppm.

General Procedure for Polymersome Preparation. Different strategies can be used to self-assemble such amphiphilic block copolymers in water, such as direct dissolution, film hydration, emulsification/diffusion, or nanoprecipitation. Due to the high glass transition and crystallinity of PBLG, we used the nanoprecipitation method. Block copolymer was then dissolved (1%) in DMSO at 55 °C and introduced into water (final concentration was 1 mg/mL). The organic solvent was then removed by dialysis (MWCO = 2000 g/mol) against Tris buffer (10 mM, 154 mM ionic strength with pH = 7.4) and the resulting polymer dispersion analyzed by dynamic light scattering (DLS).

Scheme 1. Synthetic Scheme for Formation of $PBLG_{23}$-*b*-HYA_{10} by Huisgen 1,3-Dipolar Cycloaddition, or "Click" Chemistry Coupling

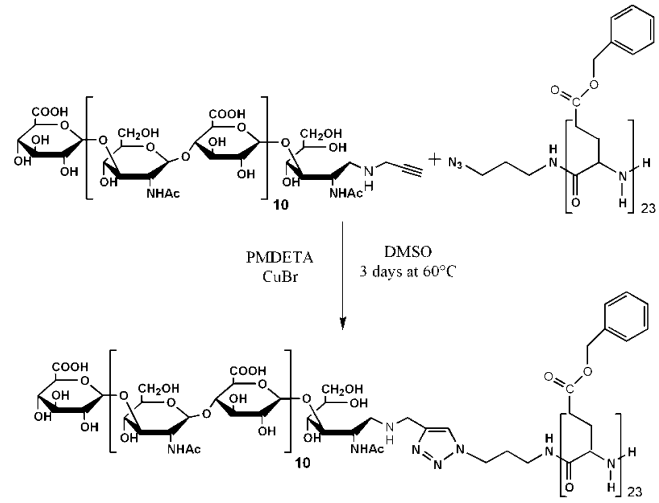

Doxorubicin Loading. Doxorubicin loading was performed at different feed weight ratios (drug: PBLG-*b*-HYA) by nanoprecipitation. Doxorubicin and block copolymer were dissolved in warm DMSO, then nanoprecipitated in Tris buffer (pH 7.5 10 mM, 154 mM ionic strength). Excess drug was removed by dialysis (4 h) against Tris buffer (MWCO: 2000 g/mol). We verified that this time was sufficient to release free doxorubicin in a controlled experiment. The doxorubicin loading content was determined as follows: the loaded vesicles were broken in a mixture (DMSO: Tris buffer (80:20)), then the sample was filtered and subjected to UV analysis at λ_{max} = 485 nm. It was checked that the absorbance of a sample without doxorubicin was negligible. Quantification was performed from the calibration curve of doxorubicin in a DMSO/Tris buffer (80:20) mixture. Each experiment was carried out in triplicate, and average values are reported in the Supporting Information file.

In Vitro Release Study. The required quantity of drug-loaded vesicles was taken in a dialysis tube (Spectra/Por Float-A-Lyzer, dialysis tubes, MWCO: 25 000 g/mol, diameter: 10 mm, volume: 10 mL). The dialysis tube (containing 5 mL of a Tris buffer solution of 100 μg/mL of free Dox or Dox-loaded polymersomes at 12 wt %) was introduced into in vitro release medium containing 50 mL Tris buffer (pH 7.5, 10 mM, 154 mM ionic strength). The whole assembly was kept at 37 ± 2 °C and covered by parafilm to avoid water evaporation. The sink conditions were maintained by replacing 2 mL of release medium with fresh media at each sampling point. The amount of drug released was estimated from the residual drug in the vesicles at each sampling point by spectrophotometry measurement at λ_{max} = 485 nm. The drug concentration was linearly related to the measured absorbance. The amount of drug released was calculated from the amount of drug initially present in the vesicles and the amount of drug retained in the vesicles at each sampling point.

Measurements. ^{1}H NMR spectra of the deprotected diblock copolymers were recorded at 60 °C on a Bruker Avance 400 MHz spectrometer using the residual proton resonance of the deuterated solvent as the internal standard.

Dynamic light scattering (DLS) experiments were performed using an ALV Laser Goniometer, which consists of 22 mW HeNe linear polarized laser with 632.8 nm wavelength and an ALV-5000/EPP Multiple Tau Digital Correlator with 125 ns initial sampling time. The

samples were kept at constant temperature (25.0 °C) during all the experiments. The accessible scattering angle range is from 10° up to 150°. The solutions were introduced into 10 mm diameter glass cells. The minimum sample volume required for the experiment was 1 mL. The data acquisition was done with the ALV-Correlator Control Software, and the counting time varied for each sample was 300 s. Water was thoroughly filtered with 0.1 μm filters and directly employed for the preparation of the solutions.

Small angle neutron scattering (SANS) experiments were performed at the Léon Brillouin Laboratory (Orphée reactor, Saclay) on the PACE spectrometer. Two spectrometer configurations have been used to cover a q range from 5×10^{-3} Å^{-1} to 0.15 Å^{-1}. The solution was introduced into a 5-mm-thick rectangular quartz cell. Data treatment was done with the PAsidur software (LLB). Absolute values of the scattering intensity ($I(q)$ in cm^{-1}) were obtained from the direct determination of the number of neutrons in the incident beam and the detector cell solid angle.

For freeze-fracture transmission electron microscopy (FF-TEM) experiments, a drop of the water solution of PBLG-*b*-HYA (0.1 mg/mL) was placed between two copper planchettes of a sandwich holder and frozen by plunging into liquid propane. The sample was then fractured at −150 °C and pressure of the order of 10^{-6} mBar in a BAF 300 Balzers apparatus. The fractured surfaces were replicated with platinum evaporated at a 45° angle, followed by carbon deposition normal to the fracture surface to increase mechanical strength. The copper planchettes were dissolved in chromerge (a mixture of chromic acid, sulfuric acid, and water). The detached replicas were then rinsed with water and cleaned from copolymer with DMSO, before being collected on a 200 mesh copper grid. Observations were made with a FEI Tecnai 12 Microscope working at 120 keV.

Atomic force microscopy (AFM) was performed under air at 25 °C using a Nanoscope IIIa microscope in tapping mode. Commercially available silicon tip probes had a spring constant of 42 N m^{-1}, a resonance frequency of 285 kHz, and a typical radius of curvature in the 8−10 nm range. Both topography and phase signal images were recorded with 512 × 512 data points. All samples were prepared on mica by spin-coating at 700 rpm for 10 min and allowed to dry for two days at room temperature.

Cell Culture. Cell culture experiments were performed on rat C6 glioma cell line, grown in Dulbecco's modified Eagle's medium (DMEM) containing 5% fetal calf serum (FCS). C6 glioma cells (5×10^5) were placed onto 10 cm diameter Falcon dishes and grown in 10 mL of DMEM cell medium with 5% FCS, penicillin (100 U/mL), streptomycin (100 μg/mL), and amphotericin B (25 μg/mL) (Invitrogen Corporation) in a water-saturated incubator at 37 °C in an atmosphere of 5% CO_2/95% air. Doxorubicin concentration in polymersomes was adjusted to be the same as free doxorubicin in whole cell line experiments.

Cell Viability. C6 cells were seeded at a density of 15×10^4 cells/well in 24 well transparent plates and incubated for 24 h. The cell viability was determined by the MTT (3-(4,5-dimethyathiazol-2-yl)-2,5-diphenyl tetrazolium bromide) assay. This assay is based on measurement of the dehydrogenase activity of viable cells by the reduction of the tetrazolium salt MTT to a blue product formazan. A stock solution of 5 mg/mL MTT was prepared in PBS, and at the designated time intervals, 10% MTT was added and incubated for 45 min at 37 °C. The medium was removed, the wells were washed once with 1 mL PBS, and cell pellets were collected in tube by centrifugation (180 *g* for 10 min). Supernatant PBS was removed and 1 mL DMSO added for solubilization of formazan by centrifugation (180 *g* for 10 min). Each sample was finally analyzed by spectrophotometry (U-2800A, Hitachi) with absorbance detection at 570 nm. Control samples were performed with untreated cell viability. In parallel, control cells were collected with a scraper and counted on a Malassez slide after Trypan blue staining.

Cell Uptake Studies (Fluorescence Microscopy). C6 cells were cultured at a density of 15×10^4 cells/well in 4 well plastic dishes (16 mm) containing 12 mm coverslips for 24 h. Free doxorubicin (5 μM) and loaded doxorubicin (5 μM) were incubated for 6 and 24 h at 37 °C in an atmosphere of 5% CO_2/95% air. After the designated time intervals, the cells were washed 2 times with PBS. The cells on coverslips were fixed 30 min with 4% paraformaldehyde (PFA) in PBS at room temperature. Coverslips were then mounted on slides with mowiol and viewed by Zeiss fluorescence microscopy (Germany).

Cell Uptake Studies (Flow Cytometry). C6 cells were cultured at a density of 15×10^4 cells/well in Petri dishes (35 mm) for 24 h. Free doxorubicin (5 μM) and loaded doxorubicin (5 μM) were incubated for 6, 24, and 48 h at 37 °C in an atmosphere of 5% CO_2/95% air. After designated time intervals, cell medium was removed and the cells were washed one time with 1 mL PBS. Cells were then scraped off with a sterile cell scraper and spun down for collection (180 *g* for 10 min). The pellet was homogeneously resuspended in 1 mL of RPMI and the cellular sample analyzed with a fluorescent assay cell sorter (FACS Calibur; Becton-Dickinson, Le Pont-De-Claix, France) working with an argon laser (emission wavelength at 488 nm). For each analysis, at least 10 000 events were counted.

Results and Discussion

To address this concept of self-targeting polymersomes, we started with the synthesis of a biocompatible polypeptide-*block*-polysaccharide copolymer, namely, a poly(γ-benzyl L-glutamate)-*block*-hyaluronan (PBLG-*b*-HYA) copolymer. A hydrophilic HYA block with a low degree of polymerization DP = 10 (polydispersity PDI = 1.4) was covalently bound to a hydrophobic PBLG segment (DP = 23, PDI = 1.1) using a Huisgen 1,3-dipolar cycloaddition, or "click" chemistry approach, which combines mild experimental conditions, tolerance of functional groups, and nearly quantitative yields,[29] according to a recently established procedure (Scheme 1).[30−32]

Here, HYA length is over the minimum HYA length of 6 to 8 saccharides required for HYA-CD44 binding interactions but too short to bind to the HARE receptor on liver endothelial cells, thus reducing the probability of systemic clearance.[31] Provided that the hyaluronan is kept in its acidic form, the block copolymer $PBLG_{23}$-*b*-HYA_{10} obtained is fully soluble in DMSO at 55 °C. Therefore, warm water was slowly added to this solution under gentle stirring in order to induce self-assembly, and DMSO was removed by dialysis. The block copolymer hydrophilic weight fraction of about 40%[3] together with the intrinsic rigidity of PBLG in helical conformation were chosen to ensure vesicle formation.[25,26] A combination of scattering techniques (DLS and SANS) and imaging methods (AFM and TEM) was used to attest the obtained vesicular morphology.

DLS experiments performed at different angles (Figure 1a) first show one main narrow relaxation time distribution with a low polydispersity of 0.08 deduced from cumulant analysis. The hydrodynamic radius R_H was calculated to be 220 nm. In addition, the linear variation of the relaxation frequency Γ vs the squared scattering vector q^2 passing through the origin is the hallmark of a translational diffusive process, confirming the presence of spherical objects (inset in Figure 1a). The sample preparation is highly reproducible and leads systematically to morphologies presenting the same R_H and polydispersity. SANS experiments were also performed in order to accurately assess the vesicular morphology (Figure 1b). The typical q^{-2} slope together with the fitting of the scattering curve with a vesicle form factor confirmed irrefutably the presence of vesicles.[32] In addition, from the slope of the representation $\ln(q^2 I(q))$ vs q (Figure 1b, inset) in the asymptotic Kratky−Porod approximation, we could estimate the thickness of the vesicles $\delta \sim 9$ nm.[35]

Assuming a bilayer structure, with PBLG blocks in α-helical conformation stacked in a strictly antiparallel orientation

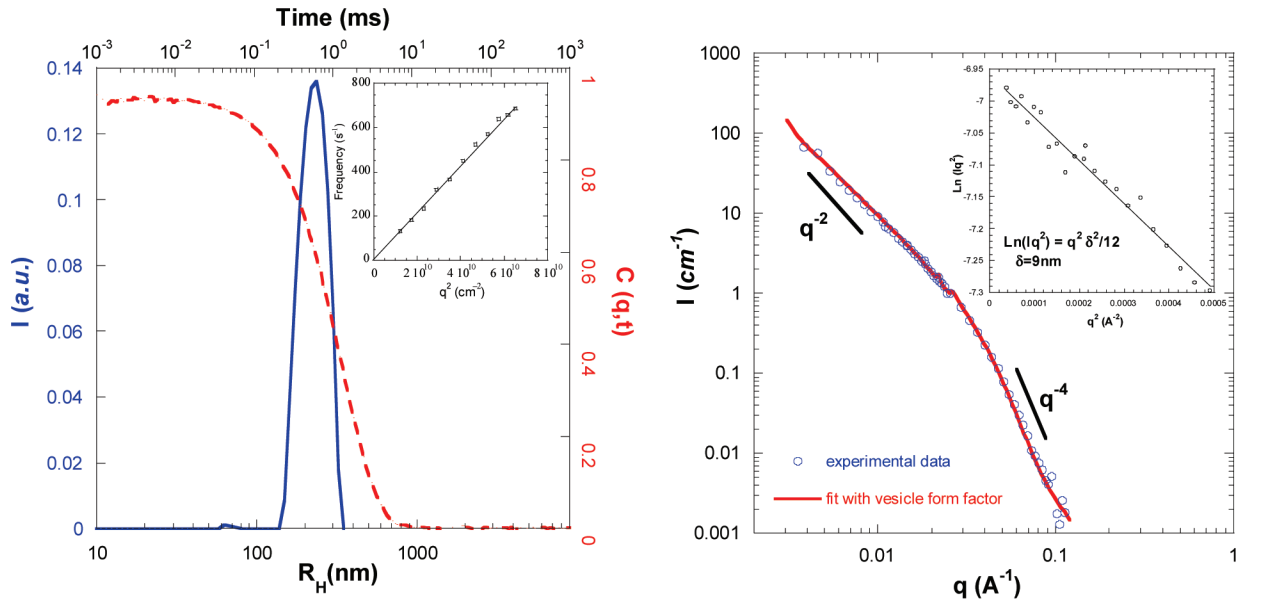

(a) (b)

Figure 1. (a) DLS autocorrelation function of the $PBLG_{23}$-*b*-HYA_{10} polymersomes and their time relaxation distribution at 90° scattering angle. The inset shows the decay rate Γ dependency to the square scattering vector q^2. (b) SANS of $PBLG_{23}$-*b*-HYA_{10} copolymer in water. Experimental data are fitted by a vesicle form factor with a radius of 220 nm and a membrane thickness δ of 9 nm.

Scheme 2. Schematic Representation of the $PBLG_{23}$-*b*-HYA_{10} Polymersomes, with a Bilayer Forming Membrane with PBLG Packed Antiparallel

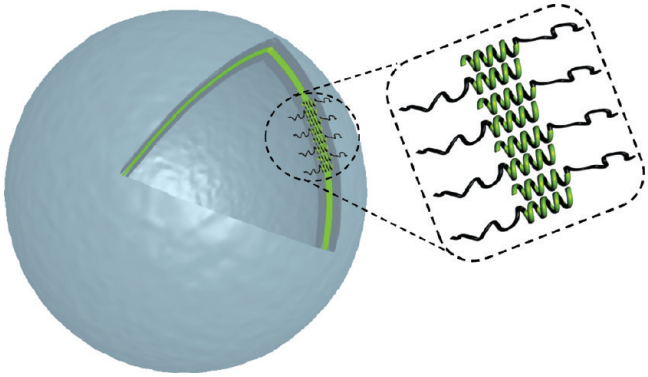

stabilizing dipolar interactions, one can calculate the expected membrane thickness to be $\delta = L_{PBLG} + 2Rg_{HYA} = 9.3$ nm (we used L_{PBLG} (nm) = 0.15 × DP and Rg_{HYA} = 2.9 nm; see Supporting Information).

The so-calculated value is in good agreement with the experimentally determined δ value from SANS. In addition, the membrane thickness is at least two times higher than that usually obtained for liposomes, ensuring a good colloidal stability upon loading and processing. A schematic representation of the polymersome structure of $PBLG_{23}$-*b*-HYA_{10} is given in Scheme 2.

The vesicle morphology has been further confirmed by TEM (Figure 2a,b) and AFM (Figure 2d,e) imaging. In particular, by AFM, one can clearly see the soft hydrophilic hyaluronan shell spreading around the polymersomes and strongly adsorbing onto the hydrophilic mica surface.

Drug loading experiments were performed on doxorubicin (Dox) as a model anticancer drug. We have chosen Dox due to its intrinsic fluorescent properties that allow us to follow the internalization mechanism and localization during in vitro experiments. Doxorubicin loading was performed at different feed weight ratios (drug/copolymer) by nanoprecipitation. The drug in excess was removed by dialysis against Tris buffer. The drug loading content and drug loading efficacy were determined by spectrophotometry. Dox loading in polymersomes was 12 ± 1 wt % (i.e., 120 μg of drug/mg of vesicles) with encapsulation efficiency of about 50%. It is worthwhile to note that the morphology and characteristic size of the vesicles remained constant after loading as illustrated in freeze-fracture TEM and AFM analysis, respectively, in Figure 2c and f. The AFM image (Figure 2f) is particularly interesting, compared to the one before loading (Figure 2d), as it shows a dense core, due to the contribution of Dox into the vesicle reservoir.

In addition, the doxorubicin-loaded polymersomes present excellent colloidal stability over several months at 4 °C with less than 10% of drug leakage after 4 months, which is crucial regarding storage stability of formulated drugs. Moreover, the solution can be freeze−dried and properly redispersed in buffer solution under stirring and gentle sonication conditions.

The release profiles of free Dox and Dox-loaded in $PBLG_{23}$-*b*-HYA_{10} polymersomes during 12 days in Tris buffer at pH 7.4 and 37 °C are illustrated in Figure 3. In comparison to the free Dox that is released after 2 h, Dox-loaded polymersomes showed a biphasic release pattern up to about 10 days, which involved an initial burst release followed by delayed release due to diffusion through the polymersome membrane. As a result, the diffusion of Dox was sustained, with about 55% cumulative drug release in 2 days.

The cytotoxicity of Dox-loaded polymersomes was evaluated in C6 glioma tumor cell lines looking at the dehydrogenase activity with the MTT assay. In addition, C6 cells are expressing CD44 receptors at their surface,[36] which should help the hyaluronan-based polymersomes internalization via endocytosis.[37] Control $PBLG_{23}$-*b*-HYA_{10} polymersomes without drug did not show a cytotoxic effect in the concentration range 0.1−700 μg/mL. Then, the effects of doxorubicin concentration as well as the incubation time was studied. It is worthwhile to mention that the doxorubicin concentration in polymersomes was adjusted to the same value as that of free drug. Table 1

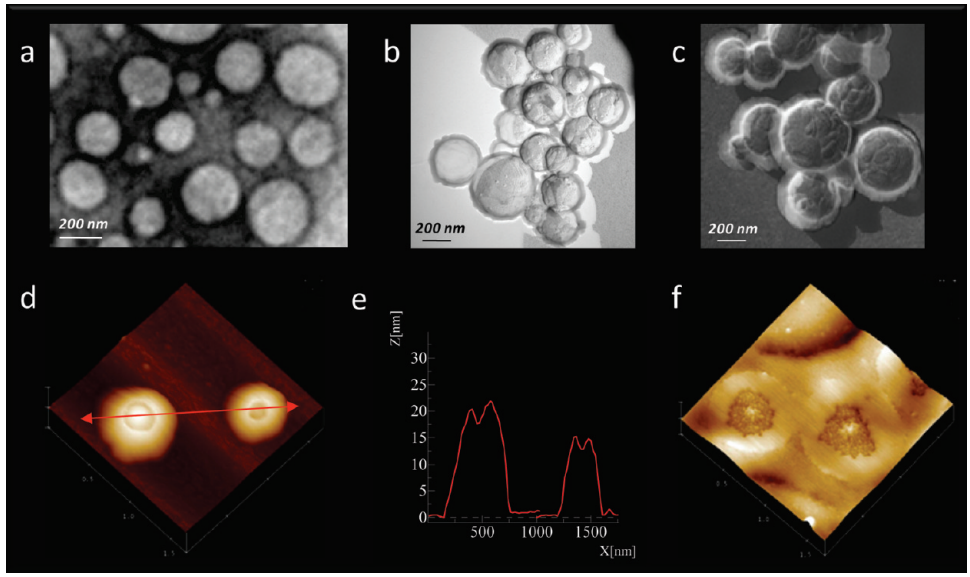

Figure 2. PBLG$_{23}$-*b*-HYA$_{10}$ polymersomes imaging from (a) TEM, (b) freeze-fracture TEM, and (d) AFM. (e) Section from AFM image d. Doxoburicin loaded polymersomes observed by (c) freeze-fracture TEM and (f) AFM.

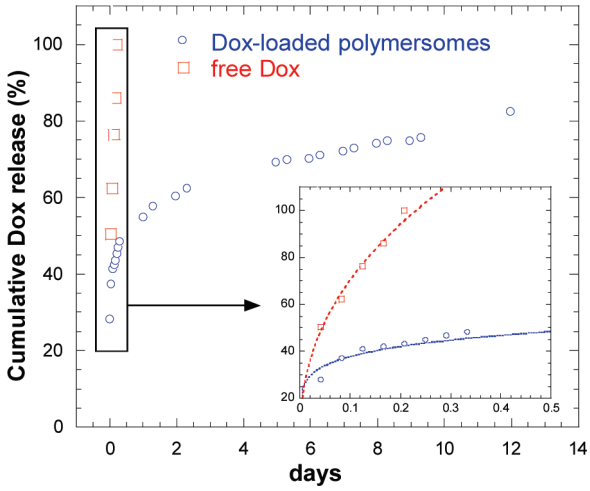

Figure 3. Release profile of free Dox and Dox-loaded polymersomes using a dialysis procedure. The same drug concentration was used (100 μg/mL) as free Dox or in Dox-loaded polymersomes (with an loading content of 12 wt %).

Table 1. In Vitro Half-Maximal Inhibitory Concentration (IC_{50}) Values Measured for Free Dox and Dox-Loaded Polymersomes on C6 Cells at Different Incubation Times

	IC_{50} (μM)	
incubation time (h)	free Dox	Dox-loaded polymersomes
24 h	20.91	[a]
48 h	1.0	7.53
72 h	0.16	2.76

[a] Value not measurable.

represents the half-maximal inhibitory concentration (IC_{50}) values of free Dox and Dox-loaded polymersomes. It is clear that IC_{50} values of free Dox and loaded Dox were time-dependent. At 48 h, free Dox produces $IC_{50} = 1$ μM whereas Dox-loaded polymersomes have $IC_{50} = 7.53$ μM. This difference could be explained by a different internalization mechanism (Figure 4) as will be explained later.

Cytotoxicity measurement at 24 h, performed at 5 μM concentration, showed that cells incubated with free Dox were strongly affected (80% death), while cells incubated with Dox-loaded polymersomes were unaffected. To gain more insight, cytotoxic cell uptake studies were performed with free and Dox-loaded vesicles (Figure 4). Indeed, after 24 h incubation with free Dox (5 μM), cells changed their morphology, being retracted and ovoid, and lost their adhesion properties (Figure 4a,c). These observations are typical for cells engaged in death processes, probably by apoptosis, as known with doxorubicin. However, for similar incubation conditions with Dox-loaded polymersomes, most of the cells still spread and stick on the culture support (Figure 4b,d). Furthermore, doxorubicin fluorescence allows for visualization of the drug distribution in the still-living cells, either by microscopy or by cytometry. After 24 h incubation, fluorescence was observed for free Dox, in the cytoplasm and mostly in the nucleus of the round cells (Figure 4c). Under the same conditions, the Dox-loaded polymersome fluorescence appeared more diffuse in the cytoplasm and particularly concentrated as dots in endosomal-like vesicles (Figure 4d inset). These images not only show that Dox-loaded vesicles are an efficient carrier to bring Doxorubicin into the cytoplasm, but also propose that the internalization mechanism of polymersomes is different from that of free Dox, which is accumulated by the cells following an unspecific diffusion process. Similar results were reported by Gao and co-workers[38] in MCF-7 cell lines with poly(ethylene oxide)-*b*-poly(ε-caprolactone) micelles. This noticeable difference at the intracellular level or in the subcellular distribution of Dox suggests that Dox-loaded polymersomes were taken up by cells mainly via an endocytic pathway. In order to further elucidate the internalization mechanism of Dox-loaded polymersomes, competitive experiments on MCF-7 human breast cancer cells, which have a high level of CD44 receptors, have been performed. Flow cytometry data revealed reduced fluorescence intensity in Dox-loaded polymersome incubated cells in the presence of free hyaluronan, but almost no effect in free doxorubicin uptake (see Supporting Information). These observations confirmed that the CD44-hyaluronan receptor−ligand interactions are at least partially contributing to the endocytosis mechanism.

The cytometry analysis, performed only on living cells, showed a similar level of cell fluorescence, independent of its intracellular location as seen by microscopy (Figure 5a). However, the large profile of fluorescence after 6 h incubation

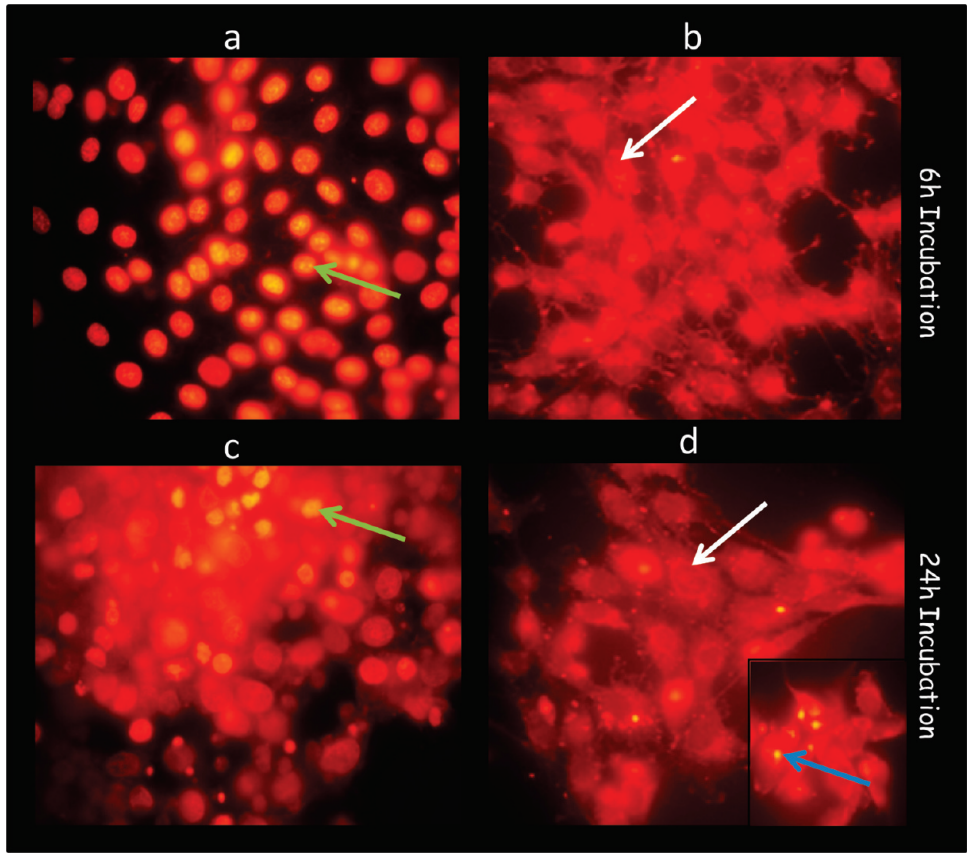

Figure 4. Fluorescence images of C6 glioma tumor cells incubated with free Dox (a,c) and Dox-loaded polymersomes (b,d) incubated for 6 h and 24 h. Green arrows show accumulation of Dox in the nucleus and DNA fragmentation. White arrows show nucleus with no or a low amount of Dox when incubated with Dox-loaded polymersomes. The blue arrow shows the accumulation of Dox-loaded polymersomes in endosomal-like cellular vesicles.

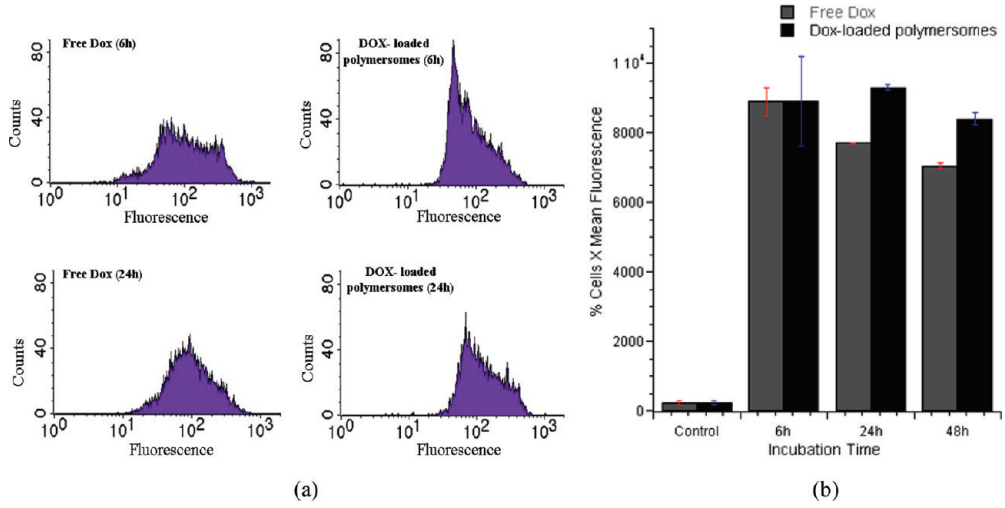

Figure 5. (a) Cytometry analysis of C6 glioma tumor cells incubated with free Dox and Dox-loaded polymersomes for 6 h and 24 h. (b) Evolution of the global fluorescence with incubation time for free Dox and Dox-loaded polymersomes. This parameter is representative of the level of the fluorescent still-living C6 population.

of free Dox is in contrast to the thinner and higher level of fluorescence measured for Dox-loaded polymersomes. This difference could be related to a diffuse intracellular repartition of doxorubicin, being located in both the cytoplasm and the nucleus for free Dox incubation (as observed by microscopy), opposed to a more localized concentration of Dox-loaded polymersomes in the cellular vesicle compartments. For the 24 h time point, the cytometry profile of free Dox incubated cells is in agreement with a nuclear accumulation. Moreover, the cell number decreased faster for cells in the free Dox conditions than for those incubated with Dox-loaded polymersomes (Figure 5b).

As a result, the time evolution of the global fluorescence per condition (Figure 5b) showed a lag of 24 h in its decrease, a consequence of the Dox-loaded polymersome compartmentalization. Indeed, this delay is representative of the time involved for the shift of the doxorubicin from the Dox-loaded vesicles, and then from endosomal-like vesicles to the cytoplasm, before

its accumulation inside the nucleus when interacting with the DNA. Then, the viability decreased in both conditions with a similar evolution. In conclusion, the internalization of the doxorubicin inside targeting polymersomes delayed the apoptosis action of the drug without affecting its efficiency due to the polymersome endosomal internalization. Finally, the cellular vesicle accumulation of Dox-loaded polymersomes strongly suggests an endocytosis pathway, probably receptor-mediated.

Conclusion

We found that block copolymers composed of a polypeptide segment and a polysaccharide moiety provide significant advantages in controlling both the vesicular structure and the biofunctionality. Such biomimetic self-assemblies combine high colloidal stability, biocompatibility, and degradability together with controlled release properties of drugs. The use of hyaluronan as the hydrophilic stabilizing block, combined with its specific ligand properties to CD44 glycoprotein receptors that are overexpressed in many cancers, provides a means to obtain synergy between structure and biofunctionality within a single material. Such an original approach opens new avenues in the preparation of multifunctional nanodevices.

Acknowledgment. This work was supported by a grant from the Science and Technology Service, Embassy of France in India, INDIA, French Ministry of Foreign affairs (MAE) for K.K.U. and from internal funds by LCPO. Authors would also thanks A. Brûlet for assistance in SANS experiments and E. Castro, O. Mondain-Monval for FF-TEM analysis. Correspondence and requests for materials should be addressed to S.L.

Supporting Information Available. Synthetic schemes, characterization by proton NMR and FTIR of the block copolymers, details about loading and release experiments, competitive cellular internalization experiments and model of the membrane packing. This material is available free of charge via the Internet at http://pubs.acs.org.

References and Notes

(1) Farokhzad, O. C.; Langer, R. *ACS Nano* **2009**, *3*, 16–20.
(2) Whitesides, G. M. *Nat. Biotechnol.* **2003**, *21*, 1161–1165.
(3) Discher, B. M.; Won, Y. Y.; Ege, D. S.; Lee, J. C. M.; Bates, F. S.; Discher, D. E.; Hammer, D. A. *Science* **1999**, *284*, 1143–1146.
(4) Ghoroghchian, P. P.; Frail, P. R.; Susumu, K.; Blessington, D.; Brannan, A. K.; Bates, F. S.; Chance, B.; Hammer, D. A.; Therien, M. J. *Proc. Natl. Acad. Sci. U.S.A.* **2005**, *102*, 2922–2927.
(5) Ahmed, F.; Pakunlu, R. I.; Srinivas, G.; Brannan, A.; Bates, F.; Klein, M. L.; Minko, T.; Discher, D. E. *Mol. Pharm.* **2006**, *3*, 340–350.
(6) Discher, D. E.; Ortiz, V.; Srinivas, G.; Klein, M. L.; Kim, Y.; Christian, D.; Cai, S.; Photos, P.; Ahmed, F. *Prog. Polym. Sci.* **2007**, *32*, 838–857.
(7) Adams, D. J.; Adams, S.; Atkins, D.; Butler, M. F.; Furzeland, S. *J. Controlled Release* **2008**, *128*, 165–170.
(8) Nasongkla, N.; Bey, E.; Ren, J.; Ai, H.; Khemtong, C.; Guthi, J. S.; Chin, S.-F.; Sherry, A. D.; Boothman, D. A.; Gao, J. *Nano Lett.* **2006**, *6*, 2427–2430.
(9) Peer, D.; Margalit, R. *Neoplasia* **2004**, *6*, 343–353.
(10) Opsteen, J. A.; Brinkhuis, R. P.; Teeuwen, R. L. M.; Loewik, D. W. P. M.; van Hest, J. C. M. *Chem. Commun.* **2007**, 3136–3138.
(11) Hammer, D. A.; Robbins, G. P.; Haun, J. B.; Lin, J. J.; Qi, W.; Smith, L. A.; Ghoroghchian, P. P.; Therien, M. J.; Bates, F. S. *Faraday Discuss.* **2008**, *139*, 129–141.
(12) Sun, G.; Fang, H.; Cheng, C.; Lu, P.; Zhang, K.; Walker, A. V.; Taylor, J.-S. A.; Wooley, K. L. *ACS Nano* **2009**, *3*, 673–681.
(13) You, L.; Schlaad, H. *J. Am. Chem. Soc.* **2006**, *128*, 13336–13337.
(14) Langer, R. *Nature* **1998**, *392*, 5–10.
(15) Peer, D.; Karp, J. M.; Hong, S.; Farokhzad, O. C.; Margalit, R.; Langer, R. *Nat. Nanotechnol.* **2007**, *2*, 751–760.
(16) Girish, K. S.; Kemparaju, K. *Life Sci.* **2007**, *80*, 1921–1943.
(17) Hu, Z.; Sun, Y.; Garen, A. *Proc. Natl. Acad. Sci. U.S.A.* **1999**, *96*, 8161–8166.
(18) Peer, D.; Margalit, R. *Int. J. Cancer,* **2004**, *108*, 780–789.
(19) Eliaz, R. E.; Szoka, F. C. *Cancer Res.* **2001**, *61*, 2592–2601.
(20) Lewanski, C. R.; Stewart, S. *Int. J. Nanomed.* **2006**, *1*, 297–315.
(21) Lewanski, C. R.; Stewart, S. *Pharm. Sci. Technol. Today* **1999**, *2*, 473–477.
(22) Bermudez, H.; Brannan, A. K.; Hammer, D. A.; Bates, F. S.; Discher, D. E. *Macromolecules* **2002**, *35*, 8203–8208.
(23) Discher, D. E.; Eisenberg, A. *Science* **2002**, *297*, 967–973.
(24) Ahmed, F.; Pakunlu, R. I.; Brannan, A.; Bates, F.; Minko, T.; Discher, D. E. *J. Controlled Release* **2006**, *116*, 150–158.
(25) Bellomo, E. G.; Wyrsta, M. D.; Pakstis, L.; Pochan, D. J.; Deming, T. J. *Nat. Mater.* **2004**, *3*, 244–248.
(26) Rodríguez-Hernández, J.; Lecommandoux, S. *J. Am. Chem. Soc.* **2005**, *127*, 2026–2027.
(27) Holowka, E. P.; Sun, V. Z.; Kamei, D. T.; Deming, T. J. *Nat. Mater.* **2007**, *6*, 52–57.
(28) Calnan, B. J.; Tidor, B.; Biancalana, S.; Hudson, D.; Frankel, A. D. *Science* **1991**, *252*, 1167–1171.
(29) Lutz, J.-F. *Angew. Chem., Int. Ed.* **2007**, *46*, 1018–1025.
(30) Schatz, C.; Louguet, S.; Le Meins, J.-F.; Lecommandoux, S. *Angew. Chem., Int. Ed.* **2009**, *48*, 2572–2575.
(31) Agut, W.; Agnaou, R.; Lecommandoux, S.; Taton, D. *Macromol. Rapid Commun.* **2008**, *29*, 1147–1155.
(32) Agut, W.; Taton, D.; Lecommandoux, S. *Macromolecules* **2007**, *40*, 5653–5661.
(33) Plat, V. M.; Szoka, F. C. *Mol. Pharm.* **2008**, *5*, 474–486.
(34) Cotton, J. P. *Neutron, X-Ray and Light Scattering*; Elsevier: North-Holland, 1991; p 19.
(35) Chécot, F.; Brûlet, A.; Oberdisse, J.; Gnanou, Y.; Mondain-Monval, O.; Lecommandoux, S. *Langmuir* **2005**, *21*, 4308–4315.
(36) Tsatas, D.; Kanagasundaram, V.; Kaye, A.; Novak, U. *J. Clin. Neurosci.* **2002**, *9*, 282–288.
(37) Palyi-Krekk, Z.; Barok, M.; Kovacs, T.; Saya, H.; Nagano, O.; Szollosi, J.; Nagy, P. *Cancer Lett.* **2008**, *263*, 231–242.
(38) Shuai, X.; Ai, H.; Nasongkl, N.; Kim, S.; Gao, J. *J. Controlled Release* **2004**, *98*, 415–426.

BM9006419